Stochastic estimation of conditional eddies in turbulent channel flow

By R. J. ADRIAN[1], P. MOIN[2,3] AND R. D. MOSER[2]

1. Background

In two recent studies, stochastic estimation algorithms were applied to numerical simulation data bases (Adrian & Moin 1987, Moin, Adrian & Kim 1987). The best (in the mean-square sense) estimate of the flow field in the vicinity of a point or points where certain data are given is the conditional average, $\langle \mathbf{u}(\mathbf{x}') \mid \mathbf{E}(\mathbf{x}) \rangle$, where $\mathbf{E}(\mathbf{x})$ denotes the data at point $\mathbf{x}$. In stochastic estimation one approximates the conditional averages by a restricted form, again determined so as to minimize mean square error. Linear stochastic estimation takes a form that is linear in the given data, $\mathbf{E}(\mathbf{x})$. In Adrian & Moin (1987), the homogeneous shear flow data base was used, and $\mathbf{E}(\mathbf{x})$ included the complete kinematic state at a point, consisting of the velocity field and the deformation tensor. In the study of Moin, *et al.* (1987), a turbulent channel flow data base was used, and $\mathbf{E}$ included only the velocity vector. In this latter study, the estimated eddy was obtained in cross-stream (y, z) planes. In both studies the probability density functions were used to specify the data, $\mathbf{E}$.

2. Multi-point stochastic estimation

The present studies contain two new elements: three- dimensional structure of *inhomogeneous* turbulence, and estimation using two-point events. The complete two-point correlation tensor, $R_{ij}(y, y', r_x, r_z)$ was recently computed by Moin & Moser (1987) from the channel-flow data base and was utilized in the present study. In addition, the stochastic estimation formulation was extended to include data at any number of points.

Consider any array of points $(\mathbf{x}_1, \mathbf{x}_2, \ldots, \mathbf{x}_n)$. The conditional averages of interest are conditional eddies defined by

$$\langle \mathbf{u}(\mathbf{x}') \mid \mathbf{u}(\mathbf{x}_1), \mathbf{u}(\mathbf{x}_2), \ldots \mathbf{u}(\mathbf{x}_N) \rangle$$

or, more briefly

$$\langle \mathbf{u}' \mid \mathbf{E} \rangle$$

where

$$\mathbf{E} = [\mathbf{v}_1 \leq \mathbf{u}_1 < \mathbf{v}_1 + d\mathbf{v}_1 \text{ and} \ldots \text{and } \mathbf{v}_N \leq \mathbf{u}_N < \mathbf{v}_N + d\mathbf{v}_N]$$

1 University of Illinois
2 NASA-Ames Research Center
3 Stanford University

is the N-point vector event consisting of $3N$ components. We wish to estimate $\langle \mathbf{u}' \mid \mathbf{E} \rangle$ as a linear function of the data $\mathbf{E}$. Nonlinear estimation usually results in a small correction (Adrian 1979, Adrian *et al.* 1987), so attention has been restricted to the linear estimate. Let us order the data vector as

$$\mathbf{E} = [u_{11}, u_{12}, u_{13}, u_{21}, \ldots, u_{N3}] = [E_1, E_2, \ldots E_{3N}]$$

The linear stochastic estimate of $\langle \mathbf{u}' \mid \mathbf{E} \rangle$ is

$$\hat{u}_i' = L_{ij} E_j. \tag{1}$$

Unless otherwise indicated, the summation convention is implied for repeated indices. Minimizing the mean square error results in the following system of equations for the estimation coefficients

$$\langle E_j E_k \rangle \, L_{ij} = \langle u_i' E_k \rangle, \qquad \begin{matrix} j,k = 1,2,\ldots,3N, \\ i = 1,2,3. \end{matrix} \tag{2}$$

In the above equation, $L_{ij} = L_{ij}(\mathbf{x}', \mathbf{x}_1, \mathbf{x}_2, \ldots \mathbf{x}_N)$ and

$$\langle u_i' E_k \rangle = R_{ij}(\mathbf{x}', \mathbf{x}_\alpha) \qquad \alpha = 1 + \mathrm{INT}(k/3), \qquad j = k - 3\alpha + 1. \tag{3}$$

3. Objective

This investigation offered the opportunity to address, for the first time, several long-standing issues regarding linear estimation and coherent structures, and to answer more completely some questions that have been addressed partially, but never with the benefit of full, three-dimensional information. The objectives were:

a. Determine how well linear estimates approximate the field obtained by true conditional averaging, using events such as those in quadrant analysis.
b. Determine the extent to which the three-dimensional linearly estimated fields correspond to coherent structures, and the degree and manner in which they differ. When is it appropriate to interpret a linear estimate as a fluid entity, and when it must be considered to be only as a smoothed mathematical entity?
c. Evaluate the type and nature of the structural information gained by employing several different types of events.
d. Learn more about the 3-D structure of important coherent motions that occur in wall turbulence.

4. Results of the investigation

The validity of the linear stochastic estimation approximation of the conditional averages has been investigated previously for different types of conditional averages by comparison of experimentally measured conditional averages with their linear estimates. While experimental comparisons have been extensive (see Adrian *et al.* 1987), they have been limited to low dimensional results. In this investigation, a full

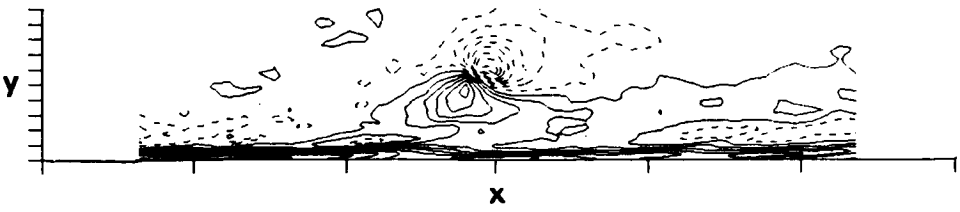

FIGURE 1. Conditional average of $\langle \omega_z'(\mathbf{x}') \mid Q2 \rangle$ using Kim and Moin (1986) $Q2$ event at $y^+ = 99$.

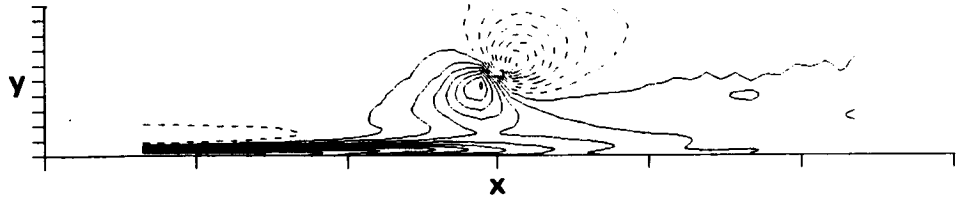

FIGURE 2. Linear stochastic estimate of $\langle \omega_z'(\mathbf{x}') \mid Q2 \rangle$ using Kim and Moin's (1986) $Q2$ event at $y^+ = 99$.

three-dimensional conditional field, determined using Kim & Moin's (1986) quadrant 2 conditional average, Figure 1, was compared to its linear estimate computed for the velocity vector $\mathbf{u}(\mathbf{x})$ conditional on the same quadrant 2 event in Figure 2. The former quantity $\langle \mathbf{u}' \mid Q2 \rangle$ is approximated in terms of the linear estimate by the following steps:

$$\langle u_i' \mid Q2 \rangle \doteq \int_{Q2} L_{ij}(\mathbf{x}, \mathbf{x}') u_j(\mathbf{x}) P(\mathbf{u}(\mathbf{x}))\, d\mathbf{u} = L_{ij}(\mathbf{x}, \mathbf{x}') \int_{Q2} u_j P(\mathbf{u}(\mathbf{x}))\, d\mathbf{u}, \quad (4)$$

where the integral extends over the range of $\mathbf{u}$ where the event $Q2 = \{u_1(\mathbf{x}) < 0,\ u_2(\mathbf{x}) < 0,\ \text{and } uv(\mathbf{x}) < 10\overline{uv}(\mathbf{x})\}$ is satisfied.

Comparison of Figures 1 and 2 shows surprisingly close agreement between the linear estimate and the conditional average. Figure 3 shows contours of the u-component velocity in channel flow conditionally averaged, given Kim & Moin's (1986) Q2 event, and comparison with the linear estimate in Figure 4, again, shows good agreement. These results, coupled with the aforementioned experimental investigation, lead us to conclude that linear estimate is a reliable approximation of the conditional average.

To study the structure of channel-flow turbulence, the first step was to identify a structure that was judged to recur frequently and to be dynamically significant. To this end, the cube of velocity data available in a velocity field was scanned to locate the positions of maximum instantaneous Reynolds stress,uv. The velocity field in the vicinity of the maximum Reynolds shear stress was surveyed by examining many

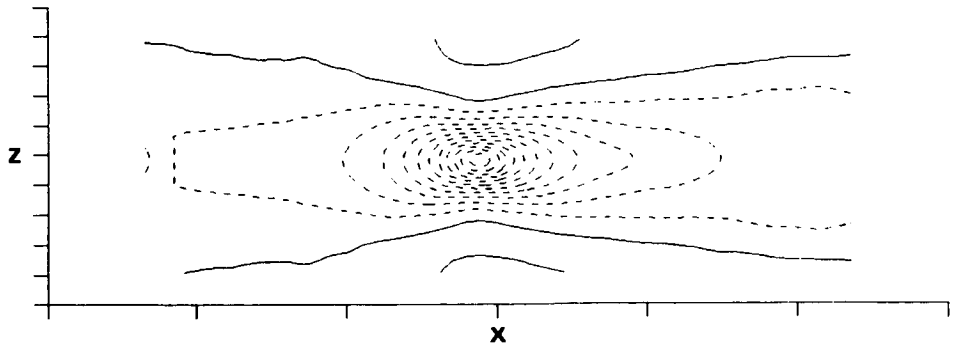

FIGURE 3. Contours of $\langle u' \mid Q2 \rangle$ in the x-z plane passing through $\mathbf{x}$ ($y^+ = 99$).

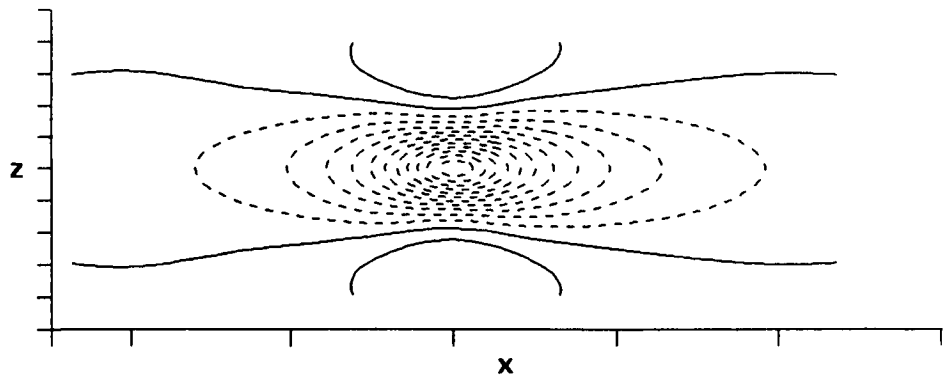

FIGURE 4. Contours of the linear estimate of $\langle u' \mid Q2 \rangle$. Same plane as in Figure 3.

different quantities in many different planes, and a reasonably complete picture of the physical structure of the flow in this region was obtained.

The structure of the flow is illustrated in Figures 5 through 10. Figures 5 and 6 show the Reynolds stress in the x-z and x-y planes. They reveal two maxima occurring at $\mathbf{x}_1 = (30, 25, 20)$ and $\mathbf{x}_2 = (35, 25, 20)$, where the numbers in the parentheses refer to grid indices. The velocities at these maxima are denoted by $\mathbf{u}_1$ and $\mathbf{u}_2$. The right-most maximum is associated with the outflow of low-momentum fluid, and the left-most maximum is associated with the inflow of high-momentum fluid. This pair of $Q2/Q4$ events is associated with a region of organized transverse vorticity, Figure 7. The velocity field in the x-y plane in the neighborhood of this point is shown in Figure 8. The vorticity ω_z is associated with a shear layer that forms between the $Q2$ and $Q4$ events. This shear layer is visible in the velocity profile of Figure 8. A cross-section of the flow in the x-z plane passing through the $Q4$ event is shown in Figure 9. In the y-z plane, it is clear that $\mathbf{x}_1$ is located on the down-wash side of a streamwise vortex. The v-component of velocity in the vicinity of the $Q2/Q4$ event is shown in Figure 10.

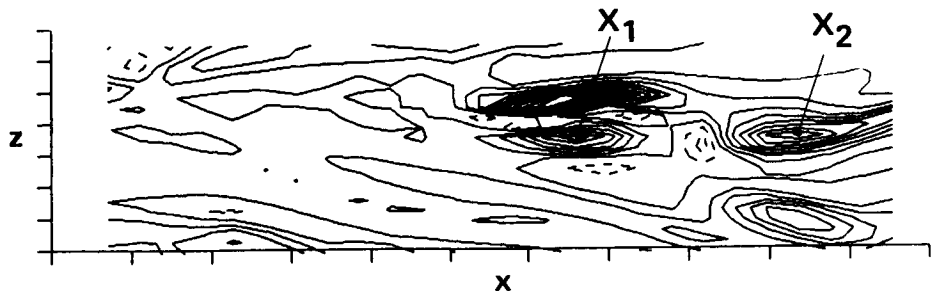

FIGURE 5. Instantaneous Reynolds shear stress contours in the x-z plane.

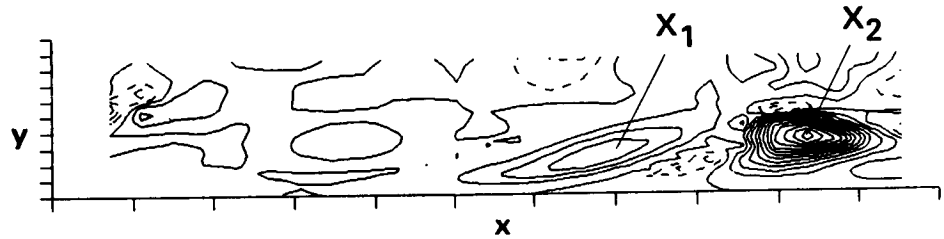

FIGURE 6. Instantaneous Reynolds shear stress contours in the x-y plane.

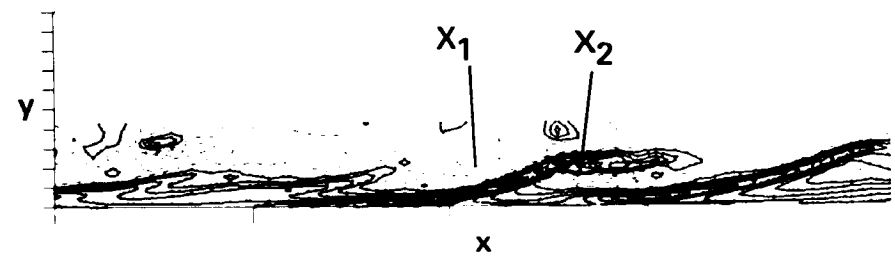

FIGURE 7. Contours of instantaneous ω_z in the x-y plane passing through $\mathbf{x}_1$.

The degree to which the linear stochastic estimate is able to represent an instantaneous structure was evaluated by picking the velocity vectors at two points, $\mathbf{x}_1$ and $\mathbf{x}_2$ centered on the $Q2$ and $Q4$ events, respectively. Using these vectors as input to the two-point linear stochastic estimator, the fluctuating velocity profile was calculated from equations (1) and (2).

Figure 11 shows contours of the linearly estimated fluctuating ω_z. There is considerable similarity between these contours and the contours of the random realization in Figure 7. A notable difference is that, in the instantaneous realization, the vorticity changes sign twice below the shear layer (see Jimenez *et al.* in this volume). Comparison of the contours of the v-component of velocity plotted in Figure 12

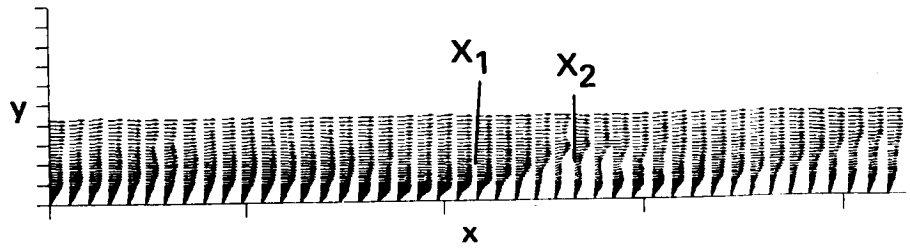

FIGURE 8. Instantaneous total velocity vectors in the x-y plane passing through $\mathbf{x}_1$.

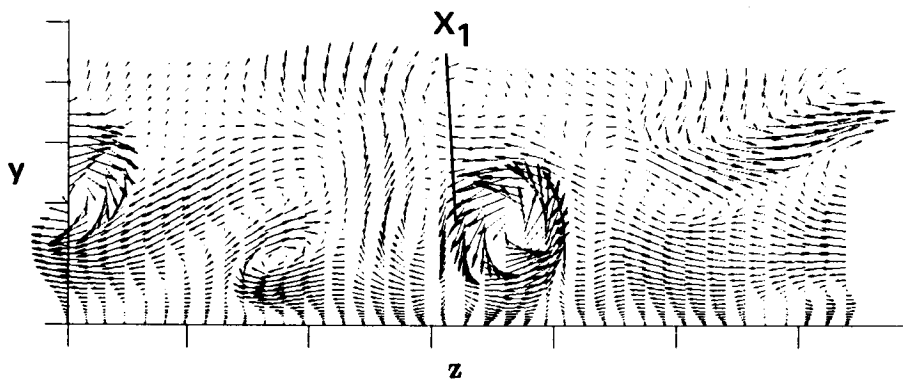

FIGURE 9. Instantaneous velocity vectors in the y-z plane passing through $\mathbf{x}_1$.

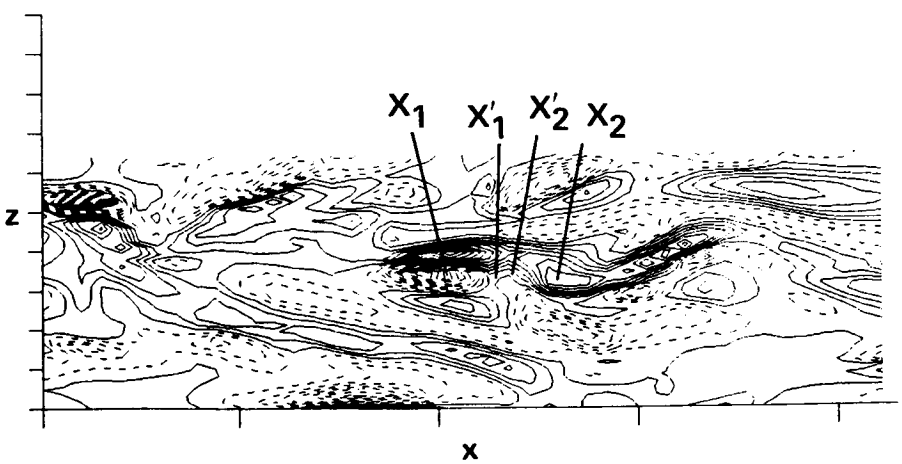

FIGURE 10. Contours of the instantaneous v-component in the x-z plane passing through $\mathbf{x}_1$ at $y^+ = 30$.

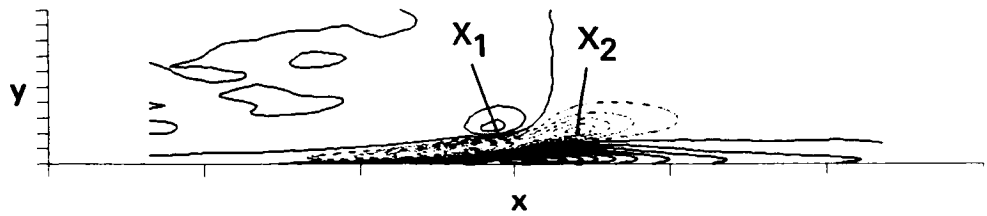

FIGURE 11. Linear estimate of the ω_z in the x-y plane through $\mathbf{x}_1$ given the $Q4$ event at $\mathbf{x}_1$ and the $Q2$ event at $\mathbf{x}_2$.

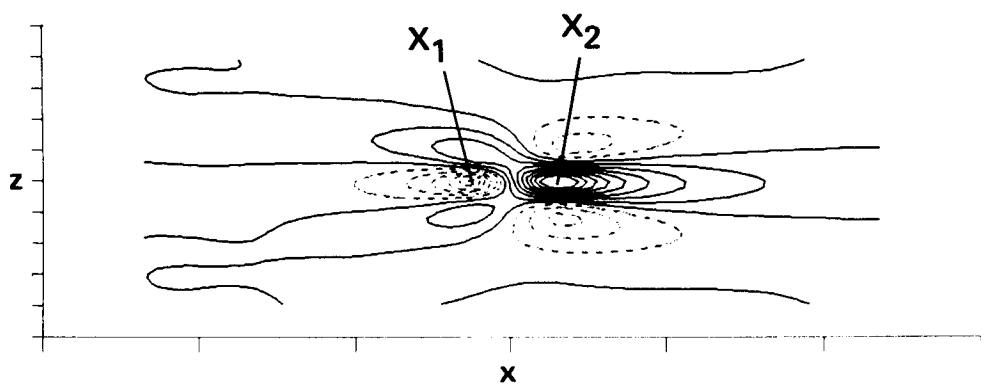

FIGURE 12. Linear estimate of v-component in the x-y plane passing through $\mathbf{x}_1$ given the $Q4$ event at $\mathbf{x}_1$ and the $Q2$ event at $\mathbf{x}_2$.

with the corresponding instantaneous contours plotted in Figure 10 is revealing. The instantaneous realizations are, of course, highly deformed, but they do reveal a region of large positive velocity surrounded by two regions of negative v-velocity in the downstream direction, and in the upstream direction an oppositely signed triplet, exactly as shown in the linear estimate. The velocity vectors in the y-z plane through $\mathbf{x}_1$, Figure 13, show a strong impingement flow with a streamwise vortex present. Note that the vortical pattern reverses sign in a plane passing through $\mathbf{x}_2$, resulting in flow away from the wall, in Figure 14.

A simplified sketch of the coherent region under investigation is shown in Figure 15. It consists of two pairs of streamwise vortices, one rotating so as to produce a $Q2$ event, i.e. low momentum fluid being pumped upwards, and the other pair lying farther upstream rotating so as to produce a $Q4$ event with high-momentum fluid being pumped downwards toward the wall. In the region between these pairs of vortices, the opposing flows of the $Q2$ and $Q4$ events generate a stagnation-point flow and an associated shear-layer tongue which has a narrow extent. This may be the origin of the region of large ω_z shown in Figures 7 and 11. It is also revealed in Figure 16, which shows (u, w) vectors in the x-z plane. It should be noted that the sketch in Figure 15 is composed of two pairs of symmetric vortices; however,

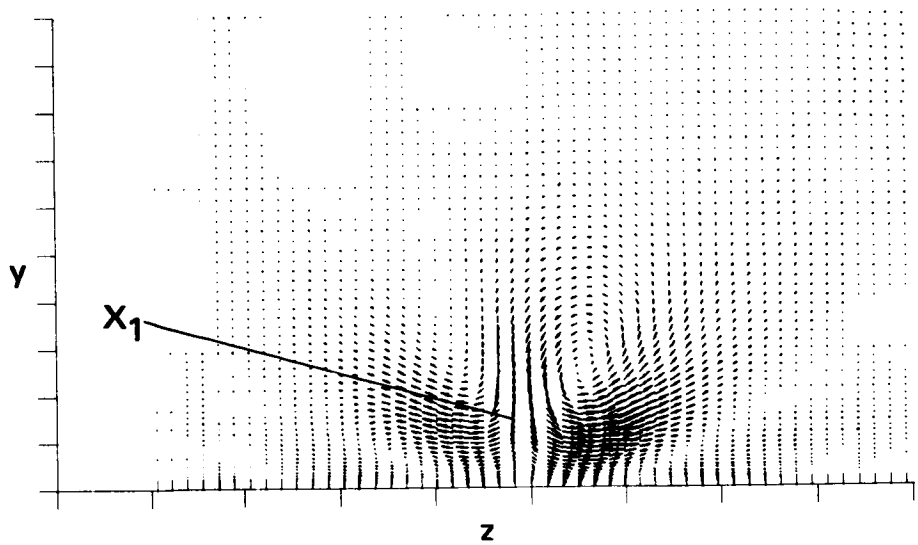

FIGURE 13. Linear estimate of (v, w) in the y-z plane passing through $\mathbf{x}_1$ given the $Q4$ event at $\mathbf{x}_1$ and the $Q2$ event at $\mathbf{x}_2$.

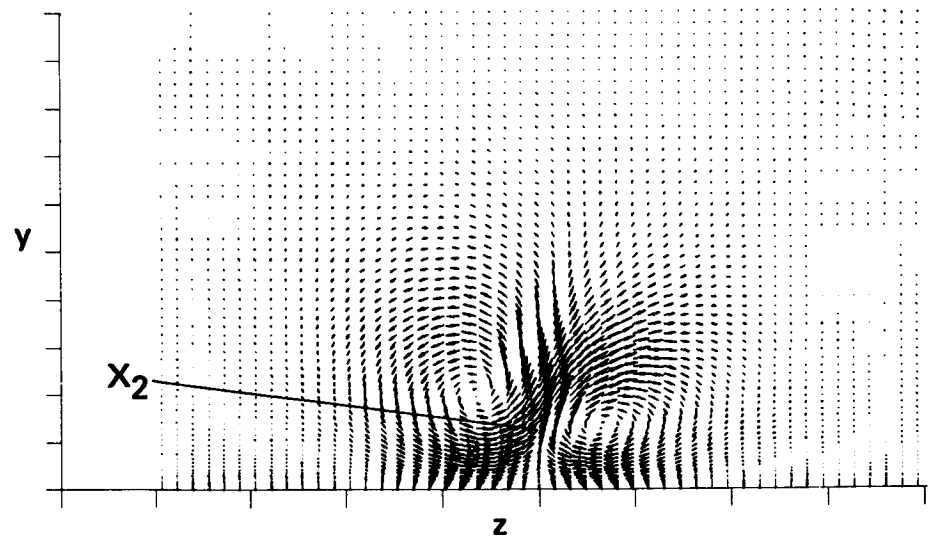

FIGURE 14. Linear estimate of (v, w) in the y-z plane passing through $\mathbf{x}_2$ given the $Q4$ event at $\mathbf{x}_1$ and the $Q2$ event at $\mathbf{x}_2$.

the instantaneous as well as the estimated flow patterns show a pronounced single vortex followed by a pair. The sketch should be viewed as a simplified average portrait of the flow.

The question arises as to the effect upon the linear stochastic estimate of selecting different points and different combinations of velocity vectors at those points. In the

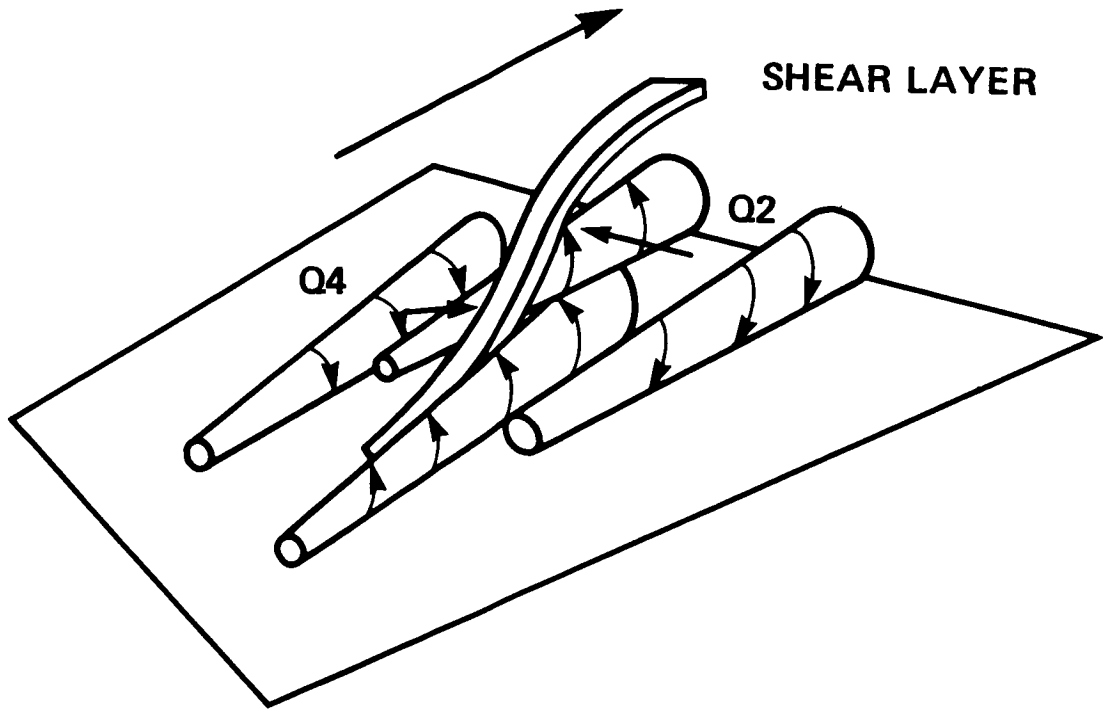

FIGURE 15. Sketch of the three-dimensional structure associated with the $Q4/Q2$ event.

preceding $Q4/Q2$ event, the events were far apart ($6\Delta x$), and they were characteristic of sweep and ejection events lying some distance away from the shear layer that they appeared to cause. Alternatively, one could concentrate on the shear layer. We chose to specify two points lying very close to the shear layer on either side of it: $\mathbf{x}_1 = (32, 26, 20)$ and $\mathbf{x}_2 = (33, 24, 20)$. We input the velocity vectors $\mathbf{u}_1$ and $\mathbf{u}_2$ taken from the instantaneous field at those points. The net effect was to specify approximately the average velocity between the points and the velocity derivatives $(\partial u_i/\partial x_j)$, since $(u_{i2} - u_{i1})/\Delta x_j$ is approximately the deformation tensor for small Δx_j.

Figure 17 shows contours of the linearly estimated v-component velocity that result from the specification of the shear event. Figure 10 shows the contours of the realization (points are marked as $\mathbf{x}_1$, $\mathbf{x}_2$). The comparison is good, but the strong lobe to the side of $\mathbf{x}_1$ is not captured.

Figure 18 shows the estimated z component of vorticity in the x-y plane. It compares well with Figure 11 for the $Q4/Q2$ event. In Figure 19, the velocity

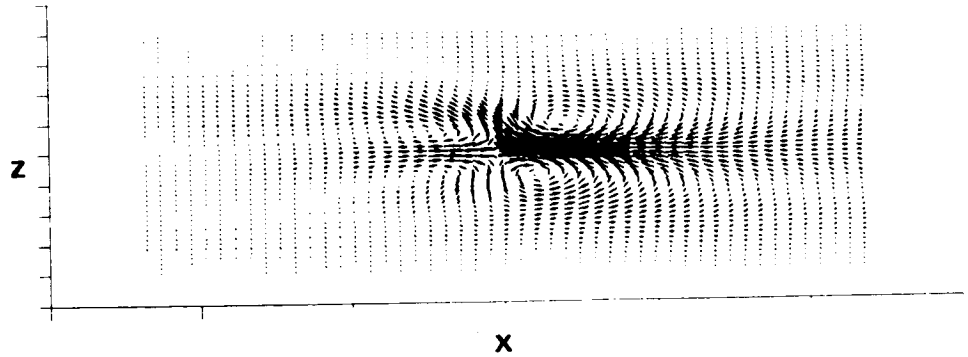

FIGURE 16. Linearly estimated (u, w) vectors in the x-z plane passing through $\mathbf{x}_1$ given the $Q4$ event at $\mathbf{x}_1$ and the $Q2$ event at $\mathbf{x}_2$.

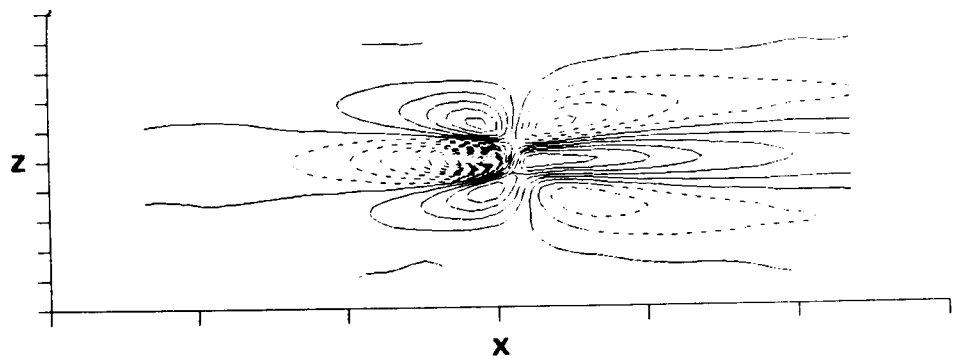

FIGURE 17. Contours of linearly estimated v-components in an x-z plane, five grid points below $\mathbf{x}_1$ ($y^+ = 21$) given the shear layer event.

vectors of the estimated eddy in the y-z plane passing through $\mathbf{x}_1$ reveal a weak pair ov counter-rotating streamwise vortices near the wall, with a single strong vortex above them.

Finally, the foregoing results each utilized information at two points in the flow. The loss of velocity information incurred when velocity at only one point was specified was also investigated. Figures 20 and 21 show that the linear estimate based on the single-point $Q2$ event at $\mathbf{x}_2 = (35, 25, 20)$ reveals only a single pair of streamwise vortices. This result suggests that two-point events provide the information needed to study the interaction between two characteristic structures.

5. Conclusion

The results of this investigation indicate that linear stochastic estimation can be used effectively in the study of numerical data bases consisting of three-dimensional vector fields, both velocity and vorticity. It is expected that pressure fields could

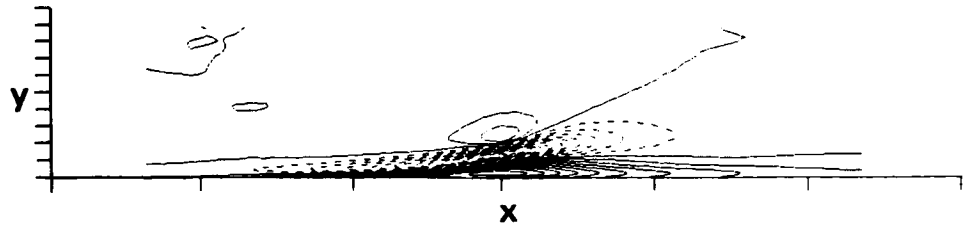

FIGURE 18. Linearly estimated ω_z in the x-y plane through $\mathbf{x}_1$ given the shear layer event.

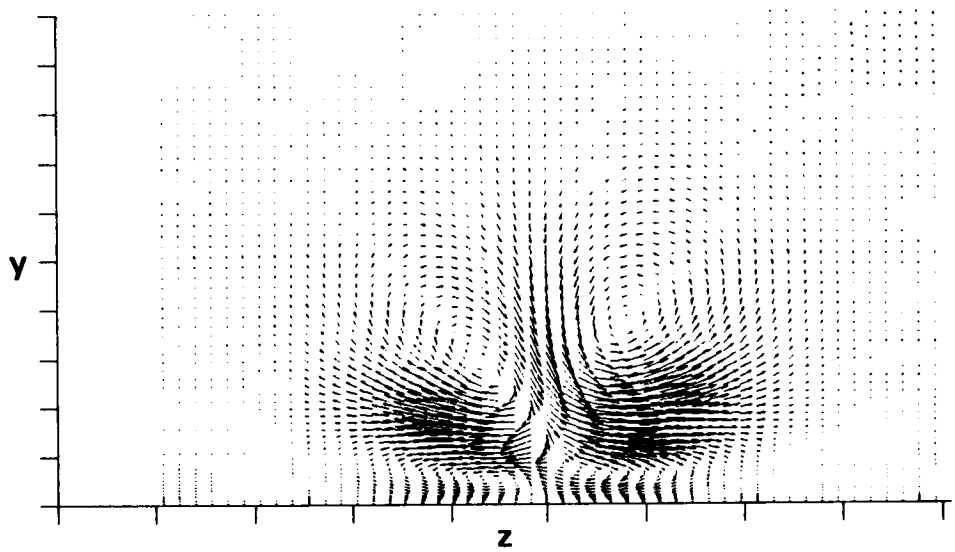

FIGURE 19. Linear estimate (v, w) in the y-z plane through $\mathbf{x}_1$ given the shear layer event.

be studied with equal facility, although this avenue has not been explored. Linear stochastic estimation is surprisingly good at approximating conditional averages, at least to the extent that the size scales and the shapes of three-dimensional structures are revealed with relatively little distortion. The linear stochastic estimate is also surprisingly good at representing instantaneous realizations of flow in the turbulent wall layer. In part, this may be a consequence of the low Reynolds number of the flow investigated, and the fact that there are strong characteristic structures in the flow. Less energetic structures may not be represented with such fidelity.

Two-point stochastic estimation yields more structural information and more detail than single-point estimation. Interestingly, the locations of the two points are not too critical, provided velocity vectors input to the stochastic estimate are those that occur within the structure. This is indicated by the fact that the stochastic estimates using distant points ($Q4/Q2$ event) and neighboring points (shear event)

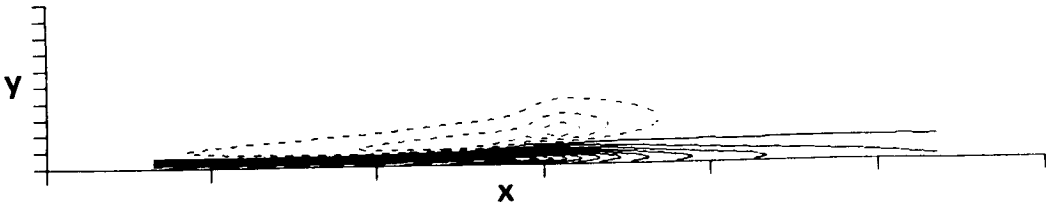

FIGURE 20. Linear estimate of ω_z in the plane through $\mathbf{x}_2$ given the single-point event $\mathbf{u}_2(\mathbf{x}_2)$.

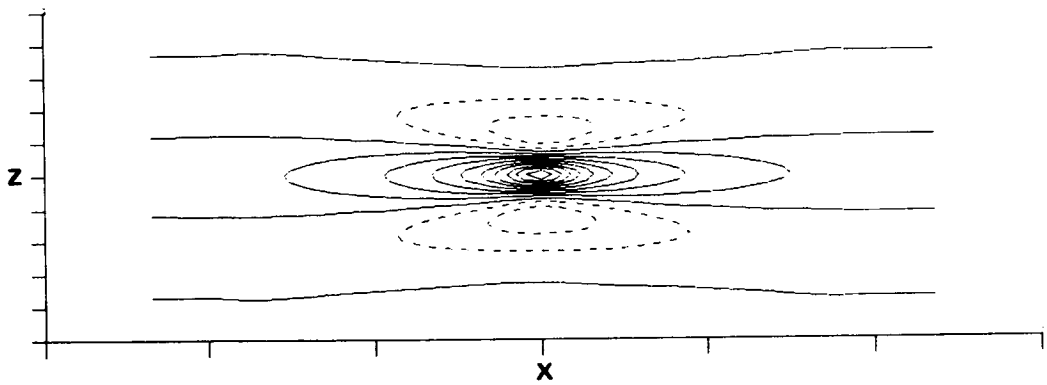

FIGURE 21. Linear estimate of v-contours in the x-z plane through $\mathbf{x}_2$ given the single-point event $\mathbf{u}_2(\mathbf{x}_2)$.

were very similar. Finally, the second point adds structural information which appears to represent interactions of flow structures in certain circumstances.

The structures we observed occurred repeatedly within the flow, but we cannot say much about their dominance or the probability of their occurrence without further systematic studies of their frequency. However, the combined $Q4/Q2$ event does appear to be associated with two pairs of streamwise vortices whose up-flows and down-flows create a stagnation point following an associated three-dimensional shear-layer tongue. Such flows can also occur as single events, i.e., $Q2$ or $Q4$ in isolation, and significant asymmetries may occur due to cross flows in the z-directions. Further work is needed to establish the three-dimensional structure of these systems.

Acknowledgments

The first author (RJA) wishes to acknowledge the generous support of the NASA/Ames-Stanford Center for Turbulence Research. Portions of this research were also supported by Grant NSF ATM 86-00509.

REFERENCES

ADRIAN, R.J. 1979 Conditional Eddies in Isotropic Turbulence. *Phys. Fluids.* **22,** 2065–2070.

ADRIAN, R.J., CHUNG, M.K., HASSAN, Y., JONES, B.G., NITHIANANDAN, C.K., & TUNG, A.T. 1987 Experimental Study of Stochastic Estimation of Turbulent Conditional Averages. 6^{th} *Turbulent Shear Flow Symposium, Toulouse, France.* Sept. 7–9, 1987, 6.1.1–6.1.7.

ADRIAN, R.J., & MOIN, P. 1987 Stochastic Estimation of Organized Turbulence Structure: Homogeneous Shear Flow. *to appear in J. Fluid Mech.*

MOIN, P., ADRIAN, R.J. & KIM, J. 1987 Stochastic Estimation of Organized Structures in Turbulent Channel Flow. 6^{th} *Turbulent Shear Flow Symposium, Toulouse, France.* Sept. 7–9, 1987.

MOSER, R. & MOIN, P. 1987 Characteristic eddy decomposition of turbulence in a channel. *to be published.*

KIM, J. & MOIN, P. 1986 The Structure of the Vorticity Field in Turbulent Channel Flow. Part 2. Study of Ensemble-Averaged Fields. *J. Fluid Mech.* **162,** 339–363.